Multiscale seismic imaging of the eastern Nankai trough by full waveform inversion

J.-X. Dessa,[1] S. Operto,[1] S. Kodaira,[2] A. Nakanishi,[2] G. Pascal,[3] J. Virieux,[1] and Y. Kaneda[2]

Received 6 May 2004; revised 26 July 2004; accepted 17 August 2004; published 23 September 2004.

[1] Classical active seismic methods fail to sharply image the earth's deep crust. We present the first crustal-scale application of 2-D full waveform inversion based on dense ocean bottom seismic data to investigate the Eastern Nankai subduction system (Japan). This approach allows to quantify seismic velocities up to an unprecedented degree of resolution. Results reveal compressive tectonic features within both the subducting oceanic crust and the backstop. At depth, velocity anomalies along major faults and structural discontinuities bring evidence for the presence of fluids and weakened material and also for a possible co-seismic slip partitioning structure. *INDEX TERMS:* 0902 Exploration Geophysics: Computational methods, seismic; 3025 Marine Geology and Geophysics: Marine seismics (0935); 8010 Structural Geology: Fractures and faults; 8105 Tectonophysics: Continental margins and sedimentary basins (1212). **Citation:** Dessa, J.-X., S. Operto, S. Kodaira, A. Nakanishi, G. Pascal, J. Virieux, and Y. Kaneda (2004), Multiscale seismic imaging of the eastern Nankai trough by full waveform inversion, *Geophys. Res. Lett.*, *31*, L18606, doi:10.1029/2004GL020453.

1. Introduction

[2] Among geophysical approaches used in crustal investigations, active seismic methods are theoretically those which best characterize and resolve structures. They are thus expected to provide an essential information on deformation mechanisms at depth. However, some serious limitations remain in that regard. In a marine environment, the deep crust is classically investigated by wide-aperture seismic experiments using networks of ocean bottom seismometers (OBS) spanning over 100–200 km in order to record upper mantle refracted waves. Resulting data are exploited through travel time inversion methods. Whether first arrivals are used alone [e.g., *Toomey et al.*, 1994] or with later reflections [e.g., *Korenaga et al.*, 2000]–the latter approach demanding a phase identification that can prove arduous and misleading in a complex medium–these techniques essentially return information on the large-scale velocity distribution. Alternatively, using the full wavefield does not require phase identification and allows significant improvement in resolution. Hence, waveform inversion based on an accurate resolution of the full wave equation should allow a breakthrough in our knowledge and understanding of deep crustal processes [*Pratt et al.*, 1996]. Three main reasons have prevented this approach from being used in deep imaging thus far: (i) it requires a densely covered acquisition over large ranges of source-receiver distances; (ii) the computational cost of full waveform modeling in large laterally-variant areas is a major obstacle; (iii) full waveform inversion is very sensitive to noise, instrument response, modeling errors, inaccuracies in the starting velocity model and the source estimation. Today, the acquisition of densely sampled wide-angle seismic data sets is developing [*Dessa et al.*, 2004]. The number of available OBSs and modern computational resources make it now possible to address the challenge of crustal-scale seismic waveform modeling.

[3] We present the first 2-D full waveform inversion of dense real OBS data to deeply image the eastern Nankai subduction system, south of Central Japan. Our approach was previously tuned on a smaller-scale experiment (C. Ravaut et al., Quantitative imaging of complex structures from multifold wide-aperture seismic data by frequency-domain full-waveform inversion: Application to a thrust belt, submitted to *Geophysical Journal International*, 2004, hereinafter referred to as Ravaut et al., submitted manuscript, 2004) and extended to the crustal imaging problem of concern here. We seek to reconstruct the P-wave velocity of target structures. The data were acquired in the frame of the Franco-Japanese SFJ-OBS survey in order to image structures in the easternmost segment of the trough, offshore Tokai district (Figure 1). This segment was the only one left unruptured after the earthquakes of 1944 and 1946 [*Kanamori*, 1972; *Ando*, 1975], making the occurrence of an important event very likely in the next decades. In spite of numerous studies, the crustal structure remains poorly imaged at depth by classical multichannel seismic acquisitions due to its tectonic complexity. Our data acquisition consisted in the deployment of a dense array of 100 OBSs along a 100 km-long profile perpendicular to the trench axis, thus providing one of the first ocean bottom multifold wide-angle marine seismic data sets. Ninety one of these OBSs provided exploitable data [*Dessa et al.*, 2004] that are considered in this study.

2. Method and Numerical Aspects

[4] Waveform modeling and inversion are both entirely implemented in the frequency domain [*Štekl and Pratt*, 1998; *Pratt et al.*, 1998]. Computational savings permitted by this approach as compared to time domain techniques is the key point for crustal-scale imaging. Only compressional

[1]UMR 6526, CNRS, Géosciences Azur, Observatoire Océanologique de Villefranche, Villefranche-sur-Mer, France.
[2]Institute for Frontier Research on Earth Evolution, Japan Marine Science and Technology Center, Yokohama, Japan.
[3]UMR 8538, CNRS, Laboratoire de Géologie, École Normale Supérieure, Paris, France.

0094-8276/04/2004GL020453$05.00

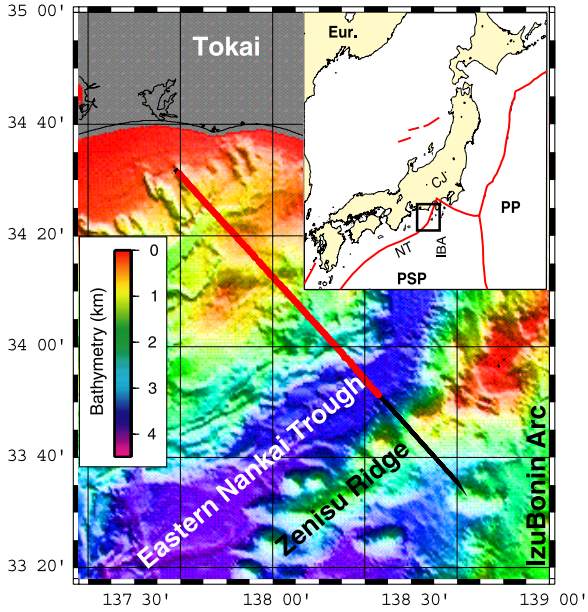

Figure 1. Survey area (framed in the inset) with the main structures referred to in the text. The straight black line and thicker coincident red line denote the seismic profile and the OBS array respectively. Eur.: Eurasia, PP: pacific plate, PSP: Philippine sea plate, CJ: central Japan, NT: Nankai trough, IBA: Izu-Bonin arc.

waves are considered–including shear waves is computationally out of reach. Solving the frequency-domain visco-acoustic full wave equation by finite differences (FD) reduces to solving a large sparse linear system whose so-called impedance matrix depends on signal frequency and model parameters and whose right hand side vector represents the seismic source [*Štekl and Pratt*, 1998]. A direct factorization method is used to solve the system because of the great efficiency offered for multisource seismic modeling. A preliminary re-ordering of the matrix strongly limits its in-fill during factorization, yielding considerable numerical gains [*Amestoy and Puglisi*, 2002]. Matrices of right hand side vectors are also used to speed up calculations.

[5] Regarding the inverse problem, frequency domain provides a natural framework to exploit redundant wavenumber coverage, thanks to wide-aperture illumination [*Sirgue and Pratt*, 2004]. This yields further numerical savings by allowing one to invert only a few selected frequencies with no loss of information. Components of increasing frequency are sequentially inverted with a linearized approach. An L2-norm cost function quantifying the misfit between observed and computed data is minimized by an iterative linearized gradient method [*Tarantola*, 1987]. The gradient is properly scaled with the diagonal elements of the approximate hessian matrix [*Shin et al.*, 2001]. Increasing frequency components are sequentially inverted, the model obtained for each frequency being used to start the inversion of the next one. This defines a multiscale approach that helps to satisfy the linearization condition (travel times must be explained within a range of

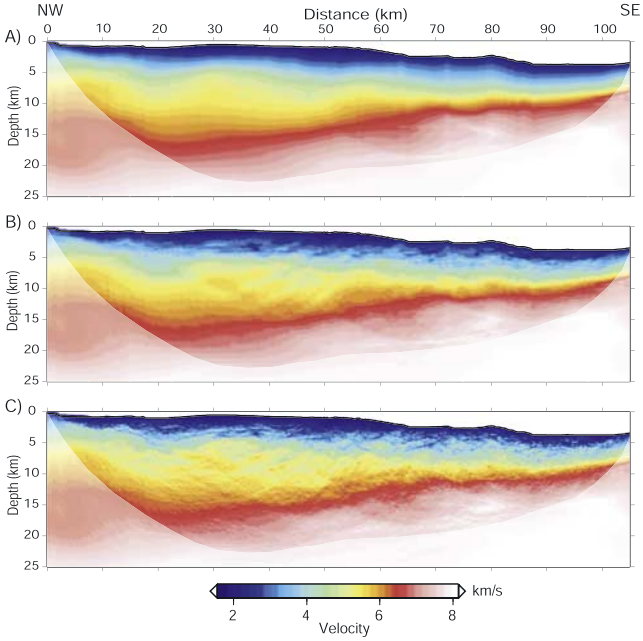

Figure 2. (A) Initial model for waveform inversion [*Dessa et al.*, 2004]. (B) Intermediate model obtained after the 3 Hz component inversion. (C) Final model obtained after inverting 13 frequency components from 3 to 15 Hz. Attenuated colors are out of first-arrival ray coverage [*Dessa et al.*, 2004].

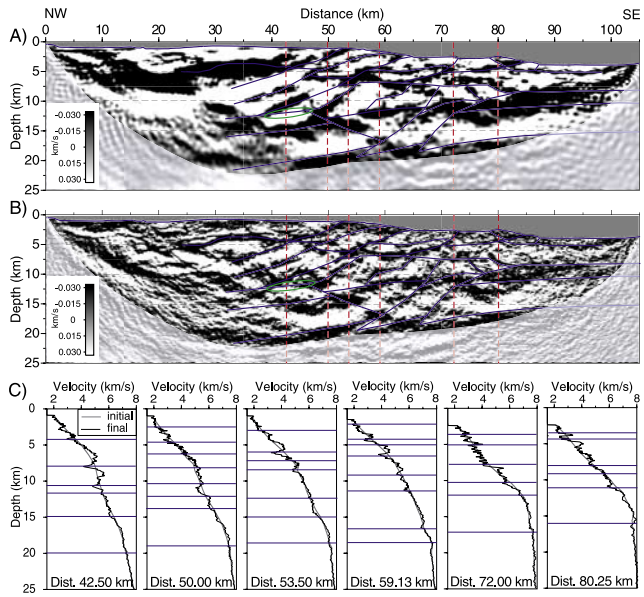

Figure 3. (A) Three Hz velocity perturbation model (i.e., slightly low-pass filtered image of the difference between corresponding waveform inversion model and the initial one) displayed with a strongly clipped scale for structural interpretation (superimposed); negative perturbations appear in black. (B) Same representation for the final perturbation model (15 Hz). (C) Velocity logs extracted from the initial and final models of Figures 2a and 2c. Horizontal blue lines are interpreted discontinuities. Green ellipses in (A) and (B) indicate a reflector whose validity is argued in the electronic supplements. The paler area is unconstrained. Note that true-amplitude velocity variations are assessed in (C); the clipped scale in (A) and (B) is not representative of absolute perturbations.

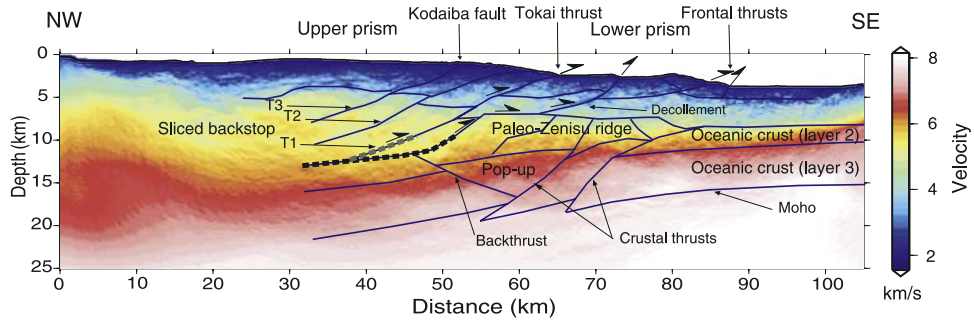

Figure 4. Interpretation of structures along the eastern Nankai trough superimposed to our final model. The thick black dashed line represents the upper part of the coseismic slip zone likely to be activated during the next Tokai earthquake. The thick gray dashed line marks a splay fault branching on the plate contact and continuing upward, along the backstop thrust T1 and eventually, the Tokai thrust. T1, T2 and T3 denote the thrusts slicing the backstop.

half a period). The initial model for the first frequency was derived by first arrival tomography [*Dessa et al.*, 2004].

[6] Thirteen frequencies were inverted between 3 and 15 Hz, producing quantitative images of increasing resolution (Figure 2). For each frequency, 4 to 5 iterations were performed in ~13 h on a single processor of a NEC-SX5 vector computer. The model size is 105 × 25 km (4201 × 1001 FD grid with a 25 m gridstep). Ten Gb of RAM are required. The acquisition includes 1050 shot positions and 91 receiver positions.

[7] Preprocessing of data consists of a deconvolution (spectral whitening) and a subsequent bandpass filtering in order to remove spurious effects (source ringing, directivity etc.) [Ravaut et al., submitted manuscript, 2004; *Operto et al.*, 2004]. Multiples are removed by time windowing. The source wavelet component is linearly inverted as a preliminary step for each frequency [*Pratt*, 1999; Ravaut et al., submitted manuscript, 2004; *Operto et al.*, 2004].

3. Results and Discussion

[8] Figure 2 presents initial, intermediate and final P-wave velocity models. Perturbation models illustrate the specific and increasingly sharper contribution of waveform inversion (Figure 3). A structural interpretation of the subduction system is proposed (Figure 4). It is derived from: (i) the joint analysis of the perturbation models (Figures 3A and 3B) and of vertical velocity profiles (Figure 3C); (ii) the geological likelihood of hypotheses (compatibility between deformation structures and expected stress regime, assumption of a regular thickness of oceanic crust prior to deformation) when ambiguities exist, due to noise and artifacts. Hence, some few events that can be viewed as dubious reflectors are interpreted as necessary discontinuities and some others are discarded (Figure 3). Such a reflector is discussed in the electronic supplements[1] (uninterpreted perturbation models are also given).

[9] The fundamental new feature recovered by waveform inversion is the quantification of the velocity field up to the higher wavenumbers theoretically attainable with the deployed source. Resolution is thus dramatically improved with respect to classic travel time inversions and sharp velocity contrasts are estimated, which migration methods fail to achieve at wide angle [*Dessa et al.*, 2004]. Large-scale velocities give an insight on acoustic properties of structures and thus on their lithological nature; short wavelengths allow an analysis of tectonic discontinuities. The most striking examples of this latter point are anomalies associated with major thrusts in the backstop and at the plate contact (Figures 2, 3, and 4). These characteristic short-wavelength low velocity zones provide an evidence for the presence of lower rigidity materials. The most likely hypothesis for that is the existence of fluid circulation along fault-induced paths and the presence of gouge in damaged fault zones at depth, essentially along the seismogenic plate contact beneath the backstop. Furthermore, the estimation of these velocity variations–up to 1 km.s^{-1} (Figure 3C)–provides a much needed constraint on in situ conditions along tectonic contacts that are otherwise not accessible, except possibly through drilling.

[10] A thickened oceanic crustal structure presently colliding the backstop is visible in our images (Figures 3 and 4). Intra-oceanic shortening is made necessary here as a transition between domains of distinct deformation regimes [*Mazzotti et al.*, 1999]. The Zenisu ridge (Figure 1) is such a compressive feature [*Lallemant et al.*, 1989] and the existence of an analogous ridge (Paleo-Zenisu) has been proposed beneath the accretionary prism [*Lallemand et al.*, 1992; *Le Pichon et al.*, 1996; *Mazzotti et al.*, 2002; *Kodaira et al.*, 2003; *Martin*, 2003; *Dessa et al.*, 2004]. Our results confirm this and furthermore demonstrate the tectonic origin of this ridge by evidencing a system of major thrusts offsetting various reflectors across the whole crust. The role of overprinted volcanism along the ridge [*Martin*, 2003] therefore appears of secondary importance in the crustal thickening. The hypothesis of a serpentinized zone within the underlying mantle [*Mazzotti et al.*, 2002] appears likely; it would localize strain in an elsewhere rigid oceanic lithosphere and would be consistent with the reactivation of fracture zones west of the Izu-Bonin arc [*Bandy and Hilde*, 1983; *Mazzotti et al.*, 2002]. Within the backstop, the observation of great thrusts (T1, T2, T3 in Figure 4) is a strong evidence for a pronounced compressive episode. Most of these features are however inactive now as no topography is being created at their seafloor termination. The landwardmost thrust (T3 in Figure 4) appears as a downward continuation of the Kodaiba fault, which would thus have been a thrusting fault although now essentially dextral strike-slip [*Thoué et al.*, 1995]. Seaward, the active

[1] Auxiliary material is available at ftp://ftp.agu.org/apend/gl/2004GL020453.

Tokai thrust appears to be rooted on the T1 backstop thrust rather than on the adjacent plate contact. We propose it to act as a splay fault along which a part of the coseismic slip is taken during great subduction earthquakes [*Park et al.*, 2002]. The rest would be transferred along the plate contact itself, continued by the shallow *décollement* imaged within the sedimentary prism, in agreement with that inferred by *Martin* [2003]. Should this hypothesis be confirmed and the Tokai splay fault remain active for a sufficient period, the backstop sliver immediately seaward of it would end up in the subduction channel, providing an erosional mechanism to the observed landward retreat of the backstop on this segment of the trough [*Nakanishi et al.*, 2002]. Due to consequences of its proximity with the Izu collision zone, the Tokai segment would thus be a partially erosive margin unlike the rest of the accretionary Nankai subduction.

[11] This study shows the interest and feasibility of applying full waveform inversion to densely-sampled OBS networks in order to perform a sharp and quantitative imaging of the whole crust in a complex 2-D geological setting. Such new approach should provide an improved knowledge of deep crustal processes.

[12] **Acknowledgments.** Computations were carried out on the NEC-SX5 of IDRIS (Orsay, France). We thank P. Amestoy (ENSEEIHT-IRIT, Toulouse, France) for providing us with the numerical solver for sparse linear algebra (MA41, from Harwell Subroutine Library). The boarding crew of the R/V Kayio performed data acquisition. Discussions with P. Henry were an appreciable contribution. R. G. Pratt and another reviewer helped with thoughtful reviews. This is UMR Géosciences Azur contribution 683, CNRS, France.

References

Amestoy, P. R., and C. Puglisi (2002), An unsymmetrized multifrontal LU factorization, *SIAM J. Matrix Anal. Appl.*, *25*, 553–569.

Ando, M. (1975), Possibility of a major earthquake in the Tokai district, Japan and its pre-estimated seismotectonic effects, *Tectonophysics*, *25*, 69–85.

Bandy, W. L., and T. W. C. Hilde (1983), Structural features of the Bonin arc: Implications for its tectonic history, *Tectonophysics*, *99*, 331–353.

Dessa, J.-X., S. Operto, S. Kodaira, A. Nakanishi, G. Pascal, K. Uhira, and Y. Kaneda (2004), Deep seismic imaging of the eastern Nankai trough, Japan, from multifold ocean bottom seismometer data by combined travel time tomography and prestack depth migration, *J. Geophys. Res.*, *109*, B02111, doi:10.1029/2003JB002689.

Kanamori, H. (1972), Tectonic implications of the 1944 Tonankai and 1946 Nankaido earthquakes, *Phys. Earth Planet. Inter.*, *5*, 129–139.

Kodaira, S., A. Nakanishi, J.-O. Park, A. Ito, T. Tsuru, and Y. Kaneda (2003), Cyclic ridge subduction at an inter-plate locked zone off central Japan, *Geophys. Res. Lett.*, *30*(6), 1339, doi:10.1029/2002GL016595.

Korenaga, J., W. S. Holbrook, G. M. Kent, P. B. Kelemen, R. S. Detrick, H.-C. Larsen, J. R. Hopper, and T. Dahl-Jensen (2000), Crustal structure of the southeast Greenland margin from joint refraction and reflection seismic tomography, *J. Geophys. Res.*, *105*, 21,591–21,614.

Lallemand, S. E., J. Malavieille, and S. Calassou (1992), Effects of oceanic ridge subduction on accretionary wedges: Experimental modeling and marine observations, *Tectonics*, *11*, 1301–1313.

Lallemant, S., N. Chamot-Rooke, X. Le Pichon, and C. Rangin (1989), Zenisu Ridge: A deep intraoceanic thrust related to subduction, off southwest Japan, *Tectonophysics*, *160*, 151–174.

Le Pichon, X., S. Lallemant, H. Tokuyama, F. Thoué, P. Huchon, and P. Henry (1996), Structure and evolution of the backstop in the eastern Nankai trough area (Japan): Implications for the soon-to-come Tokai earthquake, *Island Arc*, *5*, 440–454.

Martin, V. (2003), Structure et tectonique du prisme d'accrétion de Nankai dans la zone Tokai par imagerie sismique en trois dimensions, Ph.D. thesis, Univ. de Paris XI, Orsay, France.

Mazzotti, S., P. Henry, X. Le Pichon, and T. Sagiya (1999), Strain partitioning in the zone of transition from Nankai subduction to Izu-Bonin collision (central Japan): Implications for an extensional tear within the subducting slab, *Earth Planet. Sci. Lett.*, *172*, 1–10.

Mazzotti, S., S. Lallemant, P. Henry, X. Le Pichon, H. Tokuyama, and N. Takahashi (2002), Intraplate shortening and underthrusting of a large basement ridge in the eastern Nankai subduction zone, *Mar. Geol.*, *187*, 63–88.

Nakanishi, A., S. Kodaira, J.-O. Park, and Y. Kaneda (2002), Deformable backstop as seaward end of coseismic slip in the Nankai trough seismogenic zone, *Earth Planet. Sci. Lett.*, *203*, 255–263.

Operto, S., et al. (2004), Quantitative imaging of complex structures from multifold wide aperture seismic data, *Geophys. Prosp.*, in press.

Park, J.-O., T. Tsuru, S. Kodaira, P. R. Cummins, and Y. Kaneda (2002), Splay fault branching along the Nankai subduction zone, *Science*, *297*, 1157–1160.

Pratt, R. G. (1999), Seismic waveform inversion in the frequency domain, part 1: Theory and verification in a physical scale model, *Geophysics*, *64*, 888–901.

Pratt, R. G., Z.-M. Song, P. R. Williamson, and M. Warner (1996), Two-dimensional velocity models from wide-angle seismic data by wavefield inversion, *Geophys. J. Int.*, *124*, 323–340.

Pratt, R. G., C. Shin, and G. J. Hicks (1998), Gauss-Newton and full Newton methods in frequency-space seismic waveform inversion, *Geophys. J. Int.*, *133*, 341–362.

Shin, C., K. Yoon, K. J. Marfurt, K. Park, D. Yang, H. Y. Lim, S. Chung, and S. Shin (2001), Efficient calculation of a partial-derivative wavefield using reciprocity for seismic imaging and inversion, *Geophysics*, *66*, 1856–1863.

Sirgue, L., and R. G. Pratt (2004), Efficient waveform inversion and imaging: A strategy for selecting temporal frequencies, *Geophysics*, *69*, 231–248.

Štekl, I., and R. G. Pratt (1998), Accurate viscoelastic modeling by frequency-domain finite-differences using rotated operators, *Geophysics*, *63*, 1779–1794.

Tarantola, A. (1987), *Inverse Problem Theory: Methods for Data Fitting and Model Parameter Estimation*, Elsevier Sci., New York.

Thoué, F., P. Huchon, and K. Kobayashi (1995), Structural style of the 34°15′N, 138°10′E depression on the middle slope of the eastern Nankai trough (October 1994, Shinkai 2000 dives), *Jpn. Mar. Sci. Technol. Cent. J. Deep Sea Res.*, *11*, 197–204.

Toomey, D. R., S. C. Solomon, and G. M. Purdy (1994), Tomographic imaging of the shallow crustal structure of the East Pacific Rise at 9°30′N, *J. Geophys. Res.*, *99*, 24,135–24,157.

J.-X. Dessa, S. Operto, and J. Virieux, UMR 6526, CNRS, Géosciences Azur, Observatoire Océanologique de Villefranche, La Darse, BP 48, F-06230 Villefranche-sur-Mer, France. (jxdessa@obs-vlfr.fr)

Y. Kaneda, S. Kodaira, and A. Nakanishi, Institute for Frontier Research on Earth Evolution, Japan Marine Science and Technology Center, Showa-machi 3175-25, Kanazawa-ku, Yokohama, 236-0001, Japan.

G. Pascal, UMR 8538, CNRS, Laboratoire de Géologie, École Normale Supérieure, 24 rue Lhomond, F-75231 Paris cedex 05, France.